miR-122/SENP1 axis confers stemness and chemoresistance to liver cancer through Wnt/β-catenin signaling

JIANBO DAI[1,2*], YAQIN HAO[3*], XUN CHEN[4], QINGSAN YU[2] and BIN WANG[1,5]

[1]Department of Hepatobiliary Surgery, The First Affiliated Hospital of Chongqing Medical University;
[2]Department of General Surgery, Nan'an District People's Hospital of Chongqing; [3]Department of Gastroenterology,
The Fifth People's Hospital of Chongqing; [4]Department of Anesthesiology, Nan'an District People's Hospital of Chongqing;
[5]Department of General Surgery, Chongqing Hospital of Integrated Traditional Chinese and Western Medicine,
Chongqing 400060, P.R. China

Abstract. The property of inherent stemness of tumor cells coupled with the development of chemoresistance results in a poor prognosis for patients with liver cancer. Therefore, the present study focused on microRNA (miR)-122, a potential tumor suppressor, the expression of which has been previously shown to be significantly decreased and negatively associated with cancer cell stemness in liver cancer. The present study aimed to identify the molecular targets of miR-122 whilst uncovering the mechanism underlying chemoresistance and stemness of HepG2 cells in liver cancer. Bioinformatics online tools, such as ENCORI, coupled with dual-luciferase reporter assays in HepG2 cells, were used to identify and validate small ubiquitin-like modifier (SUMO) specific peptidase 1 (SENP1) as a potential target of miR-122 in liver cancer. The liver cancer stem cell population was determined using sphere formation assays and flow cytometry, whilst stem cell markers (Oct3/4, Nanog, B lymphoma Mo-MLV insertion region 1 homolog and Notch1) were detected by reverse transcription-quantitative PCR. Chemoresistance, cell proliferation and migratory ability of HepG2 cells were monitored using Cell Counting Kit-8, colony formation and Transwell assays, respectively. The overexpression of miR-122 by mimic transfection led to a significant decrease in the number spheres, downregulation of stem cell marker expression, the number of CD24+ cells, drug-resistance protein levels (P-glycoprotein and multidrug resistance protein), impaired chemoresistance, proliferation and migration of HepG2 cells. The transfection of SENP1 overexpression vector resulted in contrasting functions to miR-122 mimics, by partially reversing the effects induced by miR-122 mimic transfection in HepG2 cells. Wnt/β-catenin signaling has been proven to be involved in cancer stemness and malignant behavior. Western blotting analysis in HepG2 cells showed that the expression levels of both Wnt1 and β-catenin were significantly reduced after overexpressing miR-122, but increased after overexpressing SENP1. Co-transfection with the SENP1 overexpression vector reversed the suppression induced by the miR-122 mimics on Wnt1 and β-catenin expression. Co-immunoprecipitation, SUMOylation and half-life assays showed SENP1 interacted with β-catenin and decreased the SUMOylation of β-catenin, thereby enhancing its stability. Finally, tumor xenograft analyses revealed that HepG2 cells transfected with Agomir-122 exerted significantly lower tumor initiation frequency and growth rate, and a superior response to DOX *in vivo*, compared with those transfected with Agomir NC. Taken together, data from the present study miR-122/SENP1 axis can regulate β-catenin stability through de-SUMOylation, thereby promoting stemness and chemoresistance in liver cancer.

Introduction

Liver cancer is one of the most aggressive malignancies and is responsible for ~830,000 deaths worldwide in 2020 (1). The diagnosis of this disease is typically made when the liver cancer is already at an advanced stage, rendering it unresectable since it has already spread. Therefore, surgical options are limited. In such cases, chemotherapy is the only viable option, but drug resistance remains the main hindrance to its efficacy (2). Since the property of cancer stemness is closely associated with tumor initiation, self-renewal and differentiation into bulk tumor cells, it has been proposed to be a target for cancer treatment (3). Accumulating evidence supports the notion that the stemness trait of tumors is fundamentally responsible for cancer metastasis, recurrence and chemoresistance (4,5). Various survival pathways, such as the Wnt/β-catenin and STAT3 signaling pathways, have been documented to be activated in liver cancer cells expressing CD133 (a stem

Correspondence to: Dr Bin Wang, Department of General Surgery, Chongqing Hospital of Integrated Traditional Chinese and Western Medicine, 58 Danzishi New Street, Nan'an, Chongqing 400060, P.R. China
E-mail: wangbin023@hotmail.com

*Contributed equally

cell marker), which impart resistance to chemotherapy (6). Kim *et al* (7) previously demonstrated that cancer stem cell subpopulations serve a role in chemotherapy resistance in liver cancer by increasing plasticity, an ability that allows cells to maintain stability through changes in their environment, which is associated with cellular 'stemness'. Therefore, understanding the mechanisms underlying cancer stemness and chemotherapy resistance is important for providing insights into the development of effective and prospective therapeutic strategies against liver cancer.

Over the past decades, microRNAs (miR or miRNAs) have been widely studied as potential mediators of numerous human diseases, including uremia and cancer (8). As a type of non-coding RNA that are 18-25 nucleotides length, miRNAs can suppress the transcription and subsequently the translation of target mRNAs by binding to its 3' untranslated region, which in turn lead to changes in the physiological and pathophysiological processes downstream, such as the cell cycle, differentiation and autophagy (9). miRNAs, such as miR-221, miR-106b and miR-21, have been demonstrated to be oncogenic miRNAs that can regulate the malignant behaviors of tumor cells to participate in the development and growth of liver tumors (10-12). However, numerous downregulated miRNAs have also been identified to be tumor suppressors in liver cancer, including miR-122 (13). miR-122 is the predominant miRNA expressed in the liver and accounts for >50% of the total hepatic miRNA content in adult humans (14). It has been implicated in the regulation of various biological processes in the liver, including hepatic inflammation and lipid metabolism (15,16). The downregulation of miR-122 expression has been reported to serve an oncogenic role in the liver (17). Xu *et al* (18) previously found that circulating miR-122 levels are significantly associated with the overall survival rate of patients with liver cancer, suggesting that miR-122 can be applied as a reliable prognostic marker in liver cancer. It has also been reported that circulating levels of miR-122 can be an indicator of the response to transarterial chemoembolization treatment in a patient with liver cancer (19). However, the mechanisms by which the downregulation of miR-122 can induce liver cancer remain largely unclear.

Small ubiquitin-like modifier (SUMO) protein isoforms can be reversibly linked to lysine residues that reside within specific motifs in thousands of target substrates, leading to alterations in stability, solubility, localization and interaction profile (20). SUMOylation has been previously reported to be a key form of post-translational modification involved in liver cancer progression (21,22). Therefore, in the present study, bioinformatics online tools were applied to identify the potential target genes of miR-122. The SUMOylation-related genes were selected to further analyze the respective roles and underlying mechanisms as well as miR-122 in liver cancer cell stemness and chemoresistance.

Materials and methods

Bioinformatics analysis. The encyclopedia of RNA interactomes (ENCORI; https://rnasysu.com/encori/), previously known as StarBase (version 2.0) (23), was utilized to predict the potential target genes of miR-122. Briefly, in the query page of miRNA-mRNA interactions in miRNA-Target

module, miR-122 was selected in order to browse all miR-122-target interactions. Among the potential targets, SUMOylation-related genes (SENP1, SENP2, SUMO1 and SUMO3) were selected to analyze their correlation with miR-122 in liver cancer based on the pan-cancer platform in ENCORI. Next, SENP1 was selected for further analysis, as it has the strongest negative correlation with miR-122 among the four selected genes.

Cell culture and transfections. The human liver cancer cell line HepG2 was purchased from American Type Culture Collection and was maintained in DMEM (Gibco; Thermo Fisher Scientific, Inc.) containing 10% FBS (Gibco) and 1% penicillin/streptomycin in a humidified environment of 5% CO_2 at 37°C. After cell confluence reached 80-90%, the cultured cells were digested with 0.25% trypsin (w/v) and sub-cultured at a ratio of 1:4. All cell lines were tested with MycoAlert® Mycoplasma Detection Kit (Lonza Group, Ltd.) every 3 months. Cell line verification was performed using single tandem repeats profiling before the initiation of the present study. HepG2 cells were treated with 10 μM proteasome inhibitors MG132 (MilliporeSigma) for 6 h before the *in vitro* SUMOylation assay.

Cells were divided into the following four groups after transfection: i) Negative control (NC) group, which was transfected with NC agents, namely NC mimics and/or empty vectors (pcDNA3.1 vector; Invitrogen); ii) miR-122 mimic group; iii) SENP1 overexpression group (the pcDNA3.1 vector subcloned SENP1 cDNA fragment: Forward, 5'-AAGAAG ATCTTATGGATGATATTGCTGATAGGATGAGG-3' and reverse, 5'-GCCCGTCGAACTCATCACAAGAGTTTTCGG TGGAG-3'; accession no. AF149770); and iv) miR-122 mimic + SENP1 overexpression group, which was co-transfected with the miR-122 mimic and the SENP1 overexpression vector. miR-122 mimic (5'-CAAACACCAUUGUCACACUCCA-3') and NC mimic (5'-CAGUACUUUUGUGUAGUACAA-3') (pGCMV/EGFP/miR/Blasticidin plasmid backbone, cat. no. C09002) were purchased from Shanghai GenePharma Co., Ltd. Non-transfected cells were defined as the control group. In addition, HepG2 cells were also subjected to the transfection of FLAG-SENP1 (pFlag-CMV plasmid backbone; Addgene) and Myc-β-catenin (pSB1C3 plasmid backbone; Addgene) in order to investigate the interaction between SENP1 and β-catenin. In brief, cells were seeded into six-well plates and transiently transfected with the aforementioned plasmids (empty vector and SENP1 overexpression vector, 2 μg; FLAG-SENP1 and Myc-β-catenin, 4 μg; miR-122 mimic and NC mimics, 50 nM; Agomir-122 and Agomir NC, 50 nM) using Lipofectamine 2000 (Invitrogen; Thermo Fisher Scientific, Inc.) at 37°C for 48 h according to the manufacturer's protocol. After 48 h, transfection efficiency was determined by reverse transcription quantitative PCR (RT-qPCR). Subsequent experiments were performed 48 h after transfection.

RT-qPCR. The total RNA extraction from the cells with using TRIzol® (Thermo Fisher Scientific, Inc.) and subsequent reverse transcription with the PrimeScript RT reagent (cat. no. RR037B; Takara Bio, Inc.) was performed according to the manufacturer's instructions. Afterwards, qPCR was performed using SYBR green reagent (Takara Bio, Inc.) on the 7500

Table I. Primer sequences.

Gene	Sequence (5'-3')
MicroRNA-122	Forward, ACAGTGGAGTGTGACAATG
	Reverse, TCCAGTTTTTTTTTTTTTTTCAAACAC
Sentrin-specific protease 1	Forward, TTGGCCAGAGTGCAAATGG
	Reverse, TCGGCTGTTTCTTGATTTTTGTAA
Oct3/4	Forward, CTTGCTGCAGAAGTGGGTGGAGGAA
	Reverse, CTGCAGTGTGGGTTTCGGGCA
Nanog	Forward, AATACCTCAGCCTCCAGCAGATG
	Reverse, TGCGTCACACCATTGCTATTCTTC
B lymphoma Mo-MLV insertion region 1 homolog	Forward, TGGAGAAGGAATGGTCCACTTC
	Reverse, GTGAGGAAACTGTGGATGAGGA
Notch	Forward, CCTGAGGGCTTCAAAGTGTC
	Reverse CGGAACTTCTTGGTCTCCAG
U6	Forward, CTCGCTTCGGCAGCACA
	Reverse, AACGCTTCACGAATTTGCGT
GAPDH	Forward, GAGTCAACGGATTTGGTCGT
	Reverse, TTGATTTTGGAGGGATCTC

real-time PCR system. The thermocycling conditions were as follows: Initial denaturation at 95˚C for 45 sec, followed by 40 cycles of 95˚C for 15 sec and 60˚C for 15 sec. The present study utilized U6 and GAPDH as the internal reference genes to quantify miRNA and mRNA expression, respectively, using the $2^{-\Delta\Delta Cq}$ method (24). Primer sequences used in the present study are listed in Table I.

Dual-luciferase reporter assay. The dual-luciferase reporter assay was performed to verify if miR-122 can directly bind to the SENP1 mRNA 3' untranslated region (3' UTR). Partial sequences of the SENP1 3'UTR possessing the wild-type (WT) or mutant (MUT) miR-122 targeting site were cloned into the luciferase reporter pmirGLO vector (Promega Corporation) to construct the SENP1 WT and SENP1 MUT plasmids. After constructing the indicated plasmids, HepG2 cells were co-transfected with the SENP1 WT or SENP1 MUT plasmid and the miR-122 mimic or NC mimic using Lipofectamine 2000 reagent (Invitrogen; Thermo Fisher Scientific, Inc.) at 37˚C. The final concentration of the miR-122 mimic or NC mimic was 50 nM, while that of SENP1 WT or SENP1 MUT plasmid was 2 μg. After 48 h, the luciferase activity was assessed using the dual-luciferase reporter assay kit (Promega Corporation; cat. no. E1960). Firefly luciferase activity was normalized to *Renilla* luciferase activity.

Western blotting. Transfected cells were lysed with the RIPA buffer (Beyotime Institute of Biotechnology) containing PMSF and a protease inhibitor on ice for 20 min to acquire the total proteins. After determining the concentration of the total proteins using a bicinchoninic acid kit (Thermo Fisher Scientific, Inc.), equivalent amounts of protein (30 μg protein/lane) were separated on 10% gels using SDS-PAGE and transferred onto PVDF membranes. Thereafter, the membranes were blocked with skimmed milk (5%) at room temperature for 1 h, followed by incubation with the primary antibodies at 4˚C overnight. The membranes were then rinsed twice with TBS with 0.1% Tween 20 prior to incubating with the secondary antibody at room temperature for 1 h. Finally, using an enhanced chemiluminescent substrate kit (Thermo Fisher Scientific, Inc.; cat. no. 34577), the protein bands were visualized and the intensities were measured using the Image J 6.0 software (National Institutes of Health). Protein expression levels for each sample were normalized to GAPDH. Detailed information regarding the antibodies used in the present study is listed in Table II.

Sphere forming assay. A total of 1,000 cells per well were plated into six-well ultra-low attachment plates and grown in DMEM/F12 medium (Thermo Fisher Scientific, Inc.) supplemented with 5 μg/ml insulin (MilliporeSigma), 20 ng/ml basic fibroblast growth factor (Invitrogen; Thermo Fisher Scientific, Inc.) and 20 ng/ml epidermal growth factor (Invitrogen; Thermo Fisher Scientific, Inc.). The plates were then incubated at 37˚C for 15 days. The total numbers of spheroids with a diameter >50 μm in each well were then counted using a light microscope at x100 magnification.

Flow cytometry. Anti-CD24 conjugated to phycoerythrin (PE) (5 μl/test; Thermo Fisher Scientific, Inc.; cat. no 12-0247-42) was used for the present study. After incubating in PBS with 2% FBS followed by CD24-PE antibodies at room temperature in the dark for 30 min, the labeled HepG2 cells (1x10^6 cells per aliquot of incubation) were analyzed using the BD FACSCanto II analyzer flow cytometer (BD Biosciences), and the results were analyzed using FlowJo software (version 10.8.1; FlowJo LLC).

Cell Counting kit 8 (CCK-8) assay. The transfected cells were seeded into 96-well plates at a density of 8x10^3 cells/well after being digested with 0.25% trypsin-EDTA solution (MilliporeSigma) and resuspended. After complete

Table II. Detailed information of the antibodies used in western blotting.

Antibody	Manufacturer	Cat. no.	Dilution
Sentrin-specific protease 1	ProteinTech Group, Inc.	25349-1-AP	1:2,000
Multidrug resistance protein	Beyotime Institute of Biotechnology	AF7503	1:1,000
P-glycoprotein	Beyotime Institute of Biotechnology	AF2245	1:1,000
Wnt1	Beyotime Institute of Biotechnology	AF8349	1:2,000
β-catenin	Beyotime Institute of Biotechnology	AC106	1:1,000
Flag	Sigma-Aldrich	F2555	1:250
Myc	Thermo Fisher Scientific, Inc.	PA1-981	1:2,000
GAPDH	Beyotime Institute of Biotechnology	AF1186	1:1,000
Goat anti-rabbit IgG H&L HRP conjugate secondary antibody	Thermo Fisher Scientific, Inc.	31460	1:15,000

adherence (24 h of incubation), the cells were treated with DMEM containing various concentrations of doxorubicin (DOX) (0, 5, 15 and 30 μM) or sorafenib (0, 10, 20 and 40 μM) for 24 h. The cells that had 0.1% DMSO added were used as the experimental control, whereas the wells containing only DMEM were used as the blank group. After 24 h incubation at 37°C, the medium was replaced with the CCK-8 reagent (10%, v/v, dissolved in DMEM; Dojindo Molecular Technologies, Inc.). After incubating for 2 h at 37°C, the absorbance was detected using a microplate reader at 450 nm.

Colony formation assay. The transfected cells were seeded into six-well plates at a density of 2.5×10^2 cells/well. After cultivating for 2 weeks at 37°C, the cell colonies (>50 cells) were fixed with 4% paraformaldehyde for 10 min at room temperature and stained with 1% crystal violet for 10 min at room temperature. The dishes were then gently washed, photographed and counted using a BX51 fluorescence microscope at x40 magnification (Olympus, Corporation).

Transwell assay. The migration of transfected cells was evaluated using Transwell chambers (8-μm pore size; Corning, Inc.). Briefly, 5×10^4 transfected cells were seeded into the upper chambers containing 200 μl DMEM without FBS. Simultaneously, 700 μl DMEM containing FBS was added to the lower chamber. After incubation for 24 h at 37°C, the cells remaining in the upper chamber were wiped using a cotton swab, before the cells that traversed the membrane to the lower chamber were fixed in 4% paraformaldehyde for 10 min at room temperature and stained with 0.1% crystal violet for 15 min at room temperature. The stained cells were imaged and counted using a BX51 fluorescence microscope.

Co-immunoprecipitation (Co-IP). Transfected cells were lysed with 200 μl of RIPA buffer (Beyotime Institute of Biotechnology) containing PMSF and a protease inhibitor. The lysate (800 μl) was subsequently incubated with 2 μg of antibody against SENP1 (ProteinTech Group, Inc.; cat. no 25349-1-AP), β-catenin (Beyotime Institute of Biotechnology; cat. no. AC106), Flag (MilliporeSigma; cat. no. F2555) or IgG (Abcam; cat. no. ab6715) with gentle rotation overnight at 4°C, before being subsequently incubated

with Pierce™ Protein A/G Magnetic Agarose Beads (20 μl; Thermo Fisher Scientific, Inc.; cat. no. 78609) for 2 h. The beads coupling with the immune-complexes were centrifuged for 3 min at 4°C and 200 x g to sink the agarose bead to the bottom of the tube. The supernatant was removed carefully, and the agarose beads were washed with lysis buffer before the proteins were eluted in SDS-PAGE buffer with centrifugation at 1,000 x g for 1 min at room temperature. Thereafter, eluted proteins were separated on 10% gels using SDS-PAGE. The interacting proteins were detected by western blot analysis.

In vitro SUMOylation assay. In vitro SUMOylation assays were conducted using the SUMOylation kit (Enzo Life Sciences, Inc.; cat. no. BML-UW8955) as per the manufacturer's protocols. In brief, the reaction was performed using β-catenin with a reaction mixture containing SUMO protein, SUMOylation enzyme, SUMOylation buffer and Mg-ATP for 1 h at 30°C as per kit protocol. After the incubation, protein SUMOylation was identified by immunoblotting using the anti-SUMO1 antibody (1:1,000 dilution) provided with the kit. The Goat anti-rabbit IgG H&L HRP conjugate secondary antibody (1:15,000 dilution; Thermo Fisher Scientific, Inc.; cat. no. 31460) was exploited in this assay at room temperature for 1 h.

Cycloheximide (CHX) chase assay. After 48 h post-transfection, CHX (20 μg/ml; Beyotime Institute of Biotechnology) was added to the cell medium for incubation at 37°C. At the designated time points (0, 2, 4 and 8 h), cells were collected and lysed with RIPA buffer (Beyotime Institute of Biotechnology), and the protein levels of β-catenin were detected by western blot analysis.

In vivo study. All procedures regarding animals in the present study were approved by the Institutional Animal Care and Use Committee at the Nan'an District People's Hospital of Chongqing (approval no. 2020-0925; Chongqing, China) and conducted in accordance with the AVMA guidelines. A total of 84 BALB/c nude mice (female, 6-8 weeks old, 18-22 g) from the Animal Laboratory of Chongqing Medical University were maintained under specific-pathogen-free conditions with a 12/12 h light/dark cycle, 40-60% humidity, 24-26°C

temperature conditions and free access to food and water, and allowed to acclimatize for 1 week before they were subjected to subsequent experiments.

Initially, HepG2 cells were stably transfected with either 50 nM Agomir NC (5'-UUUGUACUACACAAAAGUACUG-3') or 50 nM Agomir-122 (5'-UGGAGUGUGACAAUGGUGUUUG-3'), synthesized by Guangzhou RiboBio Co., Ltd., using Lipofectamine 2000 (Invitrogen; Thermo Fisher Scientific, Inc.) before being subcutaneously injected (suspended in PBS) into the mice. To determine the *in vivo* tumor-initiating capacity of miR-122, four dilutions of HepG2 cells with either Agomir NC or Agomir-122 (500, 5,000, 50,000, or 500,000 cells) in PBS were subcutaneously injected into the mice (eight groups, n=8/group) and allowed to grow for 4 weeks. Extreme limiting dilution analysis (ELDA) software version 5.6.1.5980 (https://bioinf.wehi.edu.au/software/elda/) (25) was utilized to calculate the tumor-initiating cell frequency.

The remaining mice were randomly divided into the following four groups (n=5/group): i) Agomir NC + saline; ii) Agomir NC + DOX; iii) Agomir-122 + saline; and iv) Agomir-122 + DOX groups. Mice from both the Agomir NC + saline and Agomir NC + DOX groups were injected with $3x10^4$ Agomir NC transfected cells before being exposed to saline or 1 mg/kg DOX twice a week in accordance with their group. Mice from both the Agomir-122 + saline and Agomir-122 + DOX groups were injected with $3x10^4$ miR-122-overexpressing HepG2 cells and received saline or 1 mg/kg DOX twice a week in accordance with their group. Tumor formation monitoring began on day 7, and tumor growth was checked every 3 days with caliper measurements. Tumor volume was calculated according to the following formula: Volume=(L x W^2)/2, where W represents the width and L represents the length. On day 25, after anesthesia with 1% sodium pentobarbital intraperitoneal injection (30 mg/kg), all mice were sacrificed by cervical dislocation and tumors were harvested for protein extraction. A comprehensive judgment on death was made by observing signs of respiration, heartbeat and pupil and nerve reflexes.

Statistical analysis. All statistical analysis was conducted using the GraphPad Prism 8.0.1 software (GraphPad Software, Inc.; Dotmatics). All experiments were repeated at least three times, and all data were presented as mean ± standard deviation. Students' unpaired t-test or one-way analysis of variance followed by Bonferroni post-hoc test was performed to analyze the difference between the groups in the present study. RNA expression correlations were analyzed by Pearson's correlation coefficients based on ENCORI online database. ELDA online software was used to calculate the cancer cell stem frequency and statistical significance was assessed using the χ^2 test. P<0.05 was considered to indicate a statistically significant difference.

Results

SENP1 is predicted and confirmed as a direct target of miR-122. An increasing number of studies support the key regulatory role of miR-122 in the progression of liver cancer (17-19). However, the mechanism underlying the regulation of miR-122 in liver cancer is still not fully revealed. Considering

that SUMOylation has been shown to play a crucial role in various processes of liver cancer (21,26,27), we speculate whether the regulatory role of miR-122 in liver cancer is partly related to SUMOylation. Based on the ENCORI database, 1,278 potential target genes of miR-122 were predicted. To explore the relationship between miR-122 and SUMOylation in liver cancer, SUMOylation-related genes (SENP1-7 and SUMO1-5) were selected for subsequent analysis, and four SUMOylation-related genes, namely SENP1, SENP2, SUMO1 and SUMO3, were predicted as the potential targets of miR-122. Among these four targets, SENP1 was found to be the gene with expression levels most correlated to miR-122 expression levels in liver cancer (r=-0.339, P<0.001; Fig. 1A), therefore, SENP1 was selected for further study. RT-qPCR demonstrated that the miR-122 mimic transfection successfully caused a significant overexpression of miR-122 in HepG2 cells (Fig. 1B). The direct binding sites between miR-122 and SENP1 mRNA 3' UTR were predicted by ENCORI (Fig. 1C). To further identify whether miR-122 directly binds to the 3'UTR of SENP1, a dual-luciferase reporter assay was performed and showed that overexpression of miR-122 inhibited the luciferase activity of the reporter gene in the WT construct but not in the SENPT-MUT construct (Fig. 1D). The expression levels of SENP1 were detected further in cells after transfecting them with either the miR-122 or NC mimics to understand the effect of miR-122 on SENP1 expression. The overexpression of miR-122 significantly led to the increase in the expression of SENP1 at both mRNA and protein levels (Fig. 1E and F), suggesting that SENP1 is a direct target of miR-122 in liver cancer cells.

Stem properties impaired by miR-122 are restored by overexpressing SENP1 in HepG2 cells. Before investigating the roles of miR-122/SENP1 in liver cancer stemness, the transfection efficiency of the SENP1 overexpression vector was evaluated by RT-qPCR and western blotting. The SENP1 mRNA expression in the SENP1 overexpression group was 6.3-fold greater compared with that of the empty vector group, and the expression of SENP1 protein also showed a similar trend (Fig. 2A and B). These results indicated that the SENP1 was successfully overexpressed in HepG2. For the sphere formation assay, the number of hepatospheres formed from HepG2 cells were found to be significantly decreased after transfection with an miR-122 mimic, but was reversed by co-transfecting with the SENP1 overexpression vector (Fig. 2C). Detection of the expression of stemness-related genes Oct3/4, Nanog, B lymphoma Mo-MLV insertion region 1 homolog and Notch1 by RT-qPCR revealed a similar tendency as the sphere formation assay, showing that the miR-122 mimic led to a significant decrease in the expression levels of Oct3/4, Nanog, B lymphoma Mo-MLV insertion region 1 homolog and Notch, while the changes were reversed by co-transfection with the SENP1 overexpression vector (Fig. 2D). Collectively, this suggests that miR-122 suppressed the stemness properties of HepG2 cells, which could be reversed by the overexpression of SENP1. To further validate these results, flow cytometry assays were performed to analyzed CD24, a known marker of liver cancer stem cells. The results demonstrated that the overexpression of miR-122 caused a significant decrease in the CD24+ cell population (Fig. 2E). By contrast, co-transfection
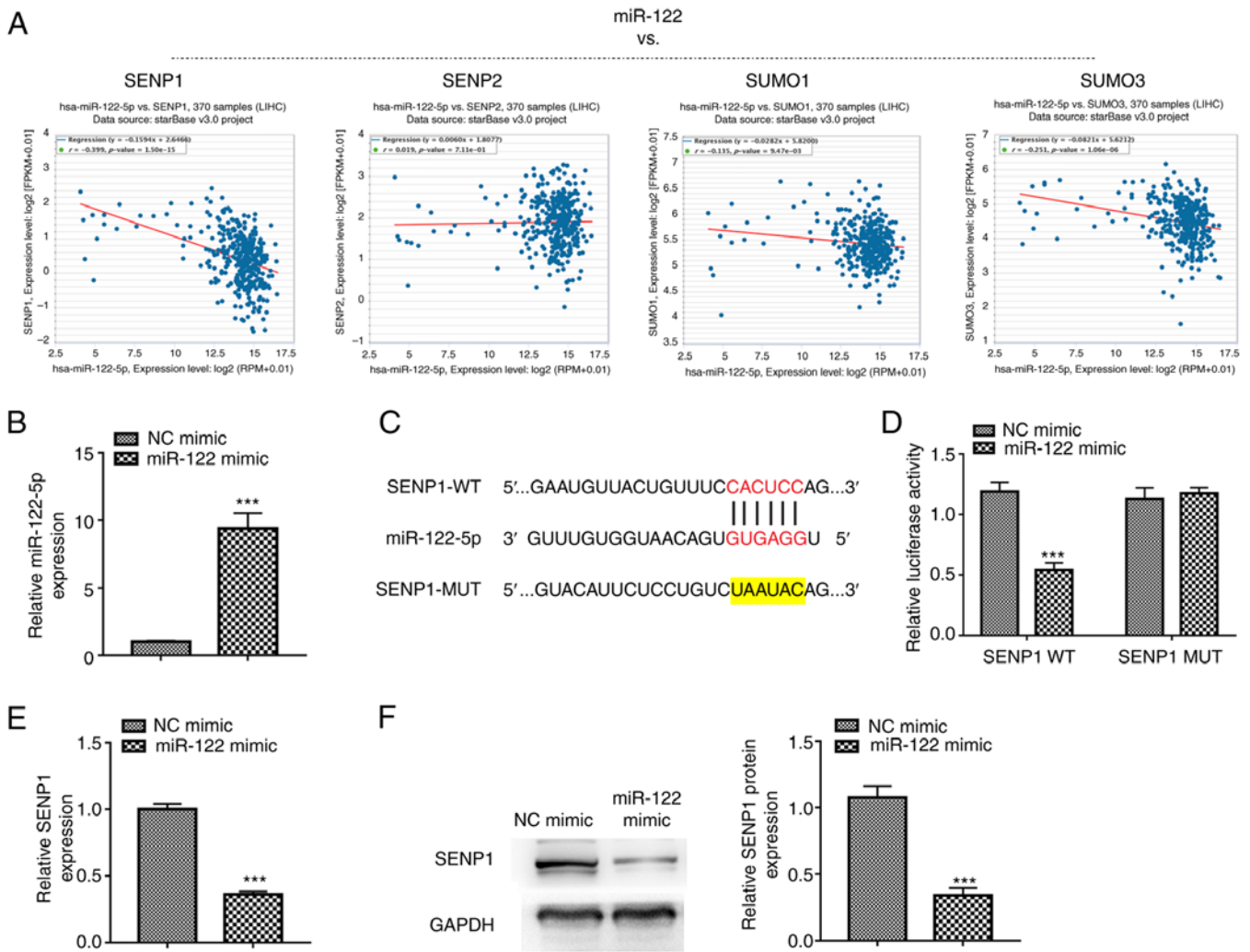
Figure 1. SENP1 is predicted and confirmed as a direct target of miR-122. (A) Correlation of miR-122 expression with SENP1, SENP2, SUMO1 and SUMO3. (B) RT-qPCR determined the expression of miR-122 in HepG2 cells after transfection with the miR-122 or NC mimic. The potential binding sites of miR-122 on the SENP1 3' untranslated region were (C) predicted by ENCORI and (D) validated by the dual-luciferase reporter assay. The mRNA and protein expression levels of SENP1 in cells transfected with miR-122 or NC mimic was detected by (E) RT-qPCR and (F) western blotting, respectively. ***$P<0.001$ vs. the NC mimic. miR, microRNA; SENP1, sentrin-specific protease 1; SENP2, sentrin-specific protease 2; SUMO1, small ubiquitin-like modifier 1; SUMO2, small ubiquitin-like modifier 2; RT-qPCR, reverse transcription-quantitative PCR.

with the SENP1 overexpression vector significantly reversed this effect (Fig. 2E). These findings suggest that miR-122 can regulate stemness properties in HepG2 cells through SENP1.

SENP1 reverses drug sensitivity in miR-122 overexpressing HepG2 cells. To address whether miR-122/SENP1 can regulate the chemoresistance of liver cancer, CCK-8, colony formation and Transwell assays were performed after treating the HepG2 cells with DOX or sorafenib (a multikinase inhibitor used as a first-line systemic treatment for liver cancer). The chemosensitivity to sorafenib and DOX in the HepG2 cells was found to be increased after transfection with miR-122 mimics, whilst SENP1 co-transfection abolished this response (Fig. 3A and B). The overexpression of miR-122 resulted in the formation of less colonies, reduced migratory ability, reduced the expression of drug-resistant P-glycoprotein (P-gp) and multidrug resistance protein in HepG2 cells (Fig. 3B-D). Conversely, SENP1 co-transfection reversed these inhibitory effects originally induced by the miR-122 mimics (Fig. 3C-E). The results of the present study suggest that the

miR-122/SENP1 axis is associated with the chemoresistance of HepG2 cells.

miR-122 regulates the Wnt/β-catenin signaling pathway through the de-SUMOylation effect of SENP1 on β-catenin. It has been frequently reported that the Wnt/β-catenin signaling pathway serves important roles in processes associated with chemoresistance and stemness (28). The role of the miR-122/SENP1 axis in the stemness and chemoresistance of HepG2 cells prompted the subsequent investigation into their potential effects on this pathway. Compared with those in the control group, the expression levels of both Wnt1 and β-catenin were significantly lower in miR-122 overexpressing cells, but higher in SENP1-overexpressing cells (Fig. 4A). Co-transfection with the SENP1 overexpression vector reversed the suppression induced by the miR-122 mimics on Wnt1 and β-catenin expression (Fig. 4A). Since SENP1 is a de-SUMOylation enzyme and the SUMOylation of β-catenin has been implicated in liver cancer growth (26), the effect of SENP1 on the SUMOylation of β-catenin and stability in
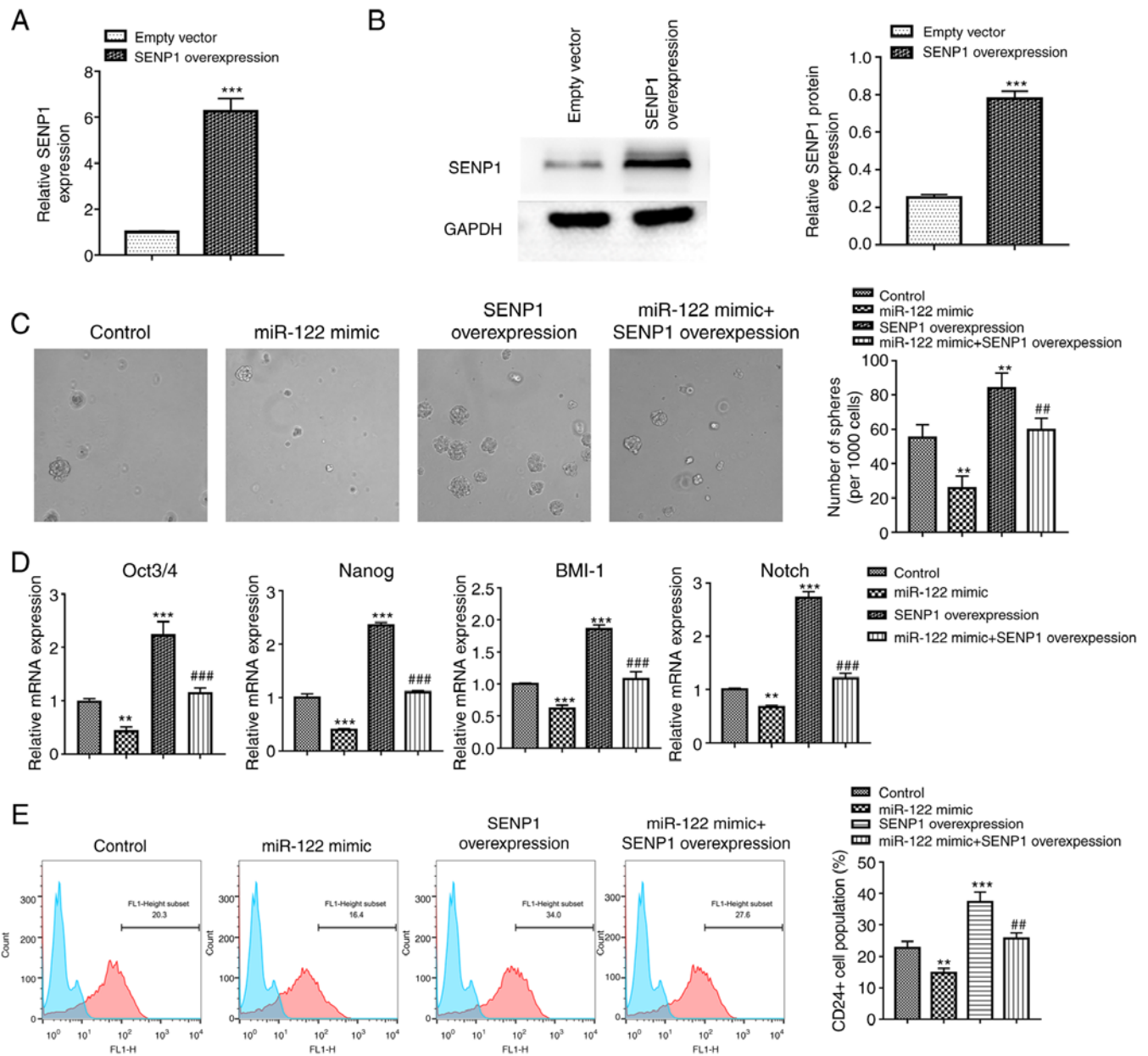
Figure 2. miR-122/SENP1 axis was involved in the stemness properties of HepG2 cells. The mRNA and protein expression levels of SENP1 in cells transfected with either the empty or SENP1 overexpression vectors was detected by (A) RT-qPCR and (B) western blotting, respectively. (C-E) HepG2 cells were transfected with the miR-122 mimic and/or SENP1 overexpression vector before the following experiments. Cells without transfection were considered as the control. (C) *In vitro* cellular self-renewal ability was evaluated using sphere formation assay. (D) The mRNA expression of stemness-related genes was analyzed by RT-qPCR. (E) The CD24+ cell population was analyzed by flow cytometry. **P<0.005 and ***P<0.001 vs. the empty vector or control; $^{##}$P<0.005 and $^{###}$P<0.001 vs. the miR-122. miR, microRNA; SENP1, sentrin-specific protease 1; BMI-1, B lymphoma Mo-MLV insertion region 1 homolog; RT-qPCR, reverse transcription-quantitative PCR.

liver cancer cells was next examined. The interaction between endogenous SENP1 and β-catenin was confirmed in HepG2 cells (Fig. 4B). Following the transfection with SENP1 or/and Myc-tagged β-catenin, the expressed FLAG-SENP1 and Myc-β-catenin were detected by the anti-FLAG and anti-Myc antibodies, further demonstrating the interaction between β-catenin and SENP1 in *in vitro* settings (Fig. 4C). After overexpressing SENP1 in cells by transfection, the levels of SUMOylation of β-catenin were markedly reduced (Fig. 4D). In addition, the half-life of β-catenin isolated from HepG2 was markedly prolonged in the SENP1 overexpressing cells (Fig. 4E). These results collectively suggest that SENP1

promotes β-catenin stability via its de-SUMOylation function, thereby regulating the Wnt/β-catenin signaling pathway.

Overexpressing miR-122 reduces liver cancer stemness and chemoresistance by downregulating SENP1/β-catenin expression in vivo. To investigate whether miR-122 can suppress the tumor initiation frequency *in vivo*, a limiting dilution experiment was performed using three different dilutions of HepG2 cells transfected with Agomir NC or Agomir-122. In total, 4 weeks after inoculation, the tumors were collected for ELDA. The results showed that the miR-122-overexpressing HepG2 cells exhibited significantly lower stem cell frequency
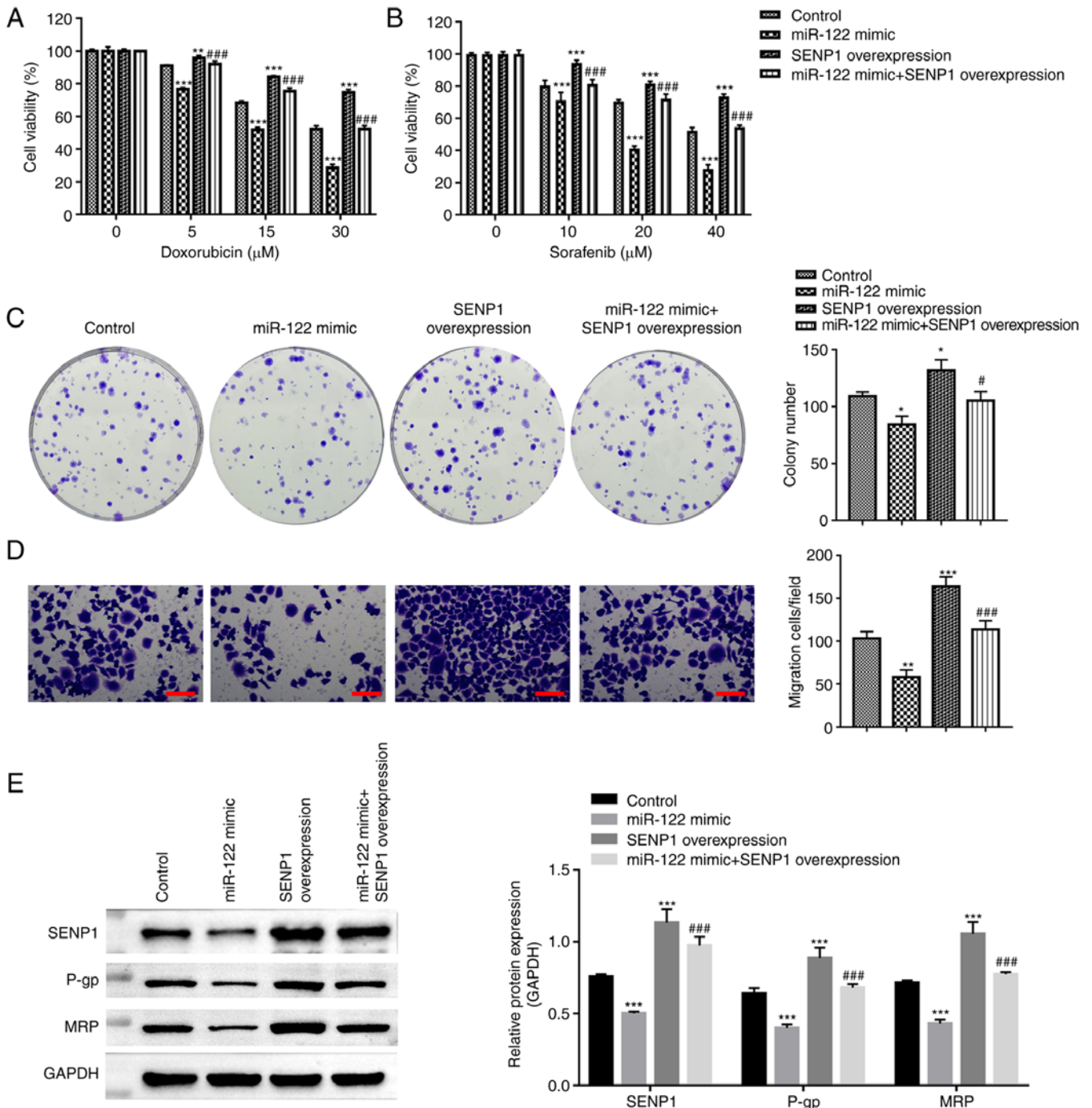
Figure 3. miR-122/SENP1 axis confers chemoresistance to HepG2 cells. HepG2 cells were transfected with the miR-122 mimic and/or SENP1 overexpression before the following experiments. Untransfected cells were considered as the control. The chemoresistance to (A) DOX and (B) sorafenib was determined by Cell Counting Kit-8 after being exposed to the different concentrations. (C) Cell proliferation and (D) migration abilities were assessed by colony formation and Transwell assays, respectively. Scale bar, 100 μm. (E) The protein expression of SENP1 and multidrug resistance associated proteins P-gp and MRP were detected by western blotting. *P<0.05, **P<0.005 and ***P<0.001 vs. the control; #P<0.05 and ###P<0.001 vs. the miR-122. miR, microRNA; DOX, doxorubicin; P-gp, P-glycoprotein; SENP1, sentrin-specific protease 1; MRP, multidrug resistance protein.

(1/70,370), compared with that in the agomir NC group (1/14,389) (Fig. 5A and B). Xenografts of the miR-122-over-expressing HepG2 cells demonstrated a lower growth rate and superior responses to DOX compared with those in the cells transfected with Agomir NC (Fig. 5C-E). The expression levels of miR-122 in the Agomir-122 group was significantly higher compared with those in the Agomir NC group (Fig. 5F). In addition, miR-122-overexpressing tumors exhibited a

significantly decreased expression levels of SENP1 and β-catenin compared with those in the control tumors (Fig. 5G), which in agreement with the *in vitro* analysis.

Discussion

As one of the most aggressive malignancies, liver cancer is the second leading cause of cancer mortality and the fifth most
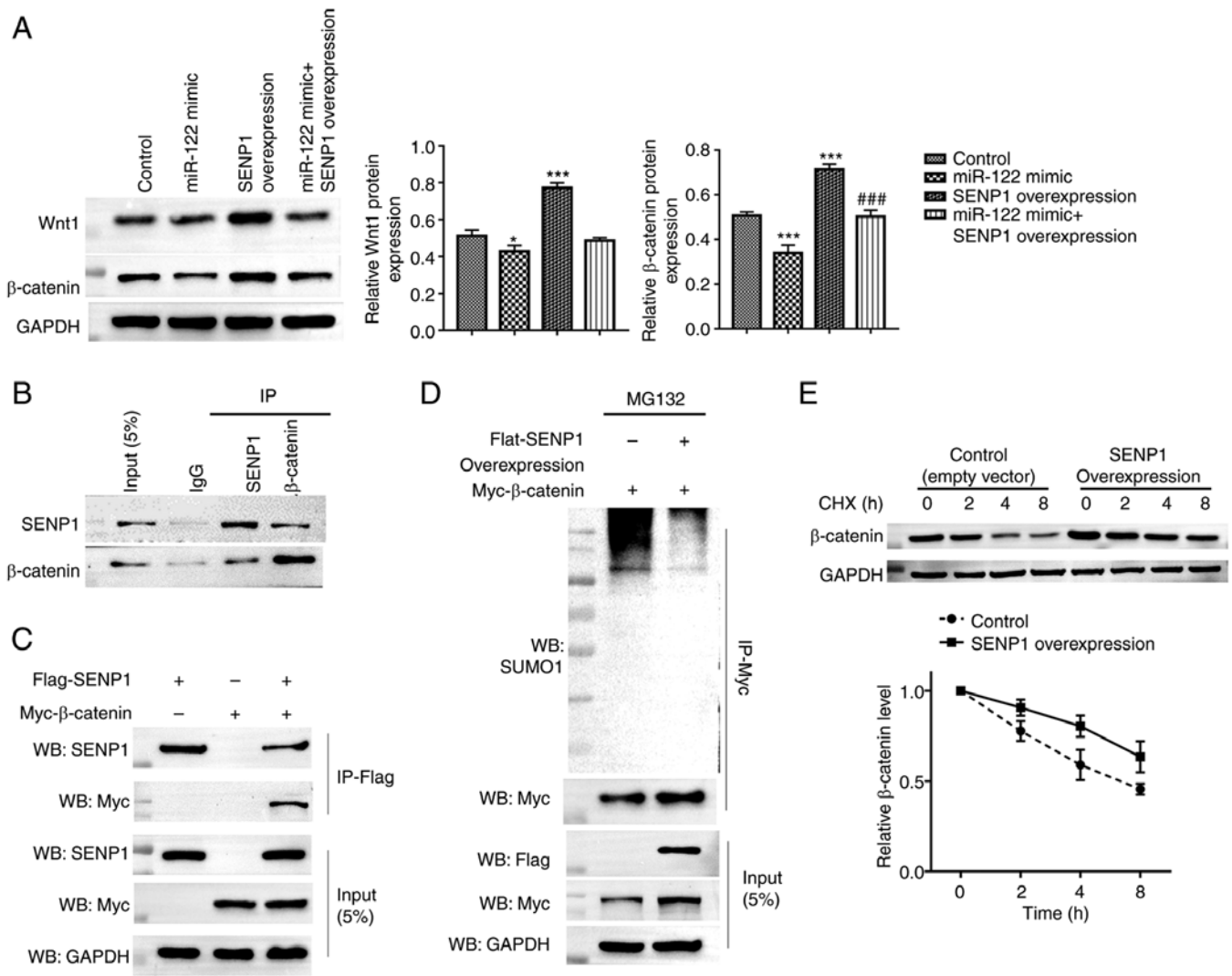
Figure 4. miR-122/SENP1 axis regulates the Wnt/β-catenin signaling pathway through the de-SUMOylation effect of SENP1 on β-catenin. (A) Western blotting was performed to measure the Wnt1 and β-catenin protein expressions in HepG2 cells transfected with the miR-122 mimic and/or SENP1 overexpression vector. Untransfected cells were considered as the control. (B) HepG2 cell lysates were immunoprecipitated with control IgG, anti-SENP1 and anti-β-catenin antibodies. The immunoprecipitates were subsequently immunoblotted with anti-SENP1 and anti-β-catenin antibodies. (C) FLAG-tagged SENP1 and/or Myc-tagged β-catenin were transfected into HepG2 cells before being lysed and immunoprecipitated with anti-FLAG antibodies. The immunoprecipitates were subsequently immunoblotted with anti-SENP1 and anti-Myc antibodies. The whole-cell lysate of HepG2 cells served as input. The lysate from HepG2 cells transfected with FLAG-tagged SENP1 or Myc-tagged β-catenin alone served as the negative control. (D) HepG2 cells were transfected with the indicated constructs and treated with MG132 for 6 h before in vitro SUMOylation assay. (E) HepG2 cells were transfected with either the empty or SENP1 overexpression vectors. After 48 h, cells were treated with CHX for 0, 2, 4 and 8 h, before being harvested, lysed and the proteins detected by western blot analysis for β-catenin. *P<0.05 and ***P<0.001 vs. the control; ###P<0.001 vs. the miR-122. miR, microRNA; SENP1, sentrin-specific protease 1; IgG, immunoglobulin G; CHX, cycloheximide.

commonly diagnosed cancer, with >410,000 new cases in China in 2020 (29). Despite the progress achieved in liver cancer therapy over the last few decades, the prognosis of patients with liver cancer remains poor (30). Therefore, potentially novel therapeutic targets for improving the clinical outcomes is of considerable importance for patients with liver cancer.

miRNAs may either serve as tumor suppressors or oncogenes in liver cancer by regulating the expression of key regulatory genes associated with cancer occurrence and progression (31). Among them, miR-122 has been identified to be a tumor suppressor miRNA in multiple malignancies, including liver cancer (17). However, the specific mechanism underlying its suppressive role in liver cancer remain to be fully elucidated.

Post-translational protein modifications, such as phosphorylation and ubiquitination, can modulate the stability, activity, interactions and subcellular localization of their target proteins, which in turn can alter subsequent biological processes. SUMOylation is another important type of reversible post-translational protein modification that is mediated by a family of ubiquitin-like small proteins (SUMO1-5), which serves to modulate protein stability and function (32). By contrast, SUMOylation can be directly reversed by a group of SENPs, which de-SUMOylate the proteins (33). Accumulating evidence has demonstrated the causal relationship between SUMOylation and liver cancer (27). The protein inhibitor of activated STAT4, a pivotal component of the TGFβ pathway, was found to be highly expressed and correlated with poor
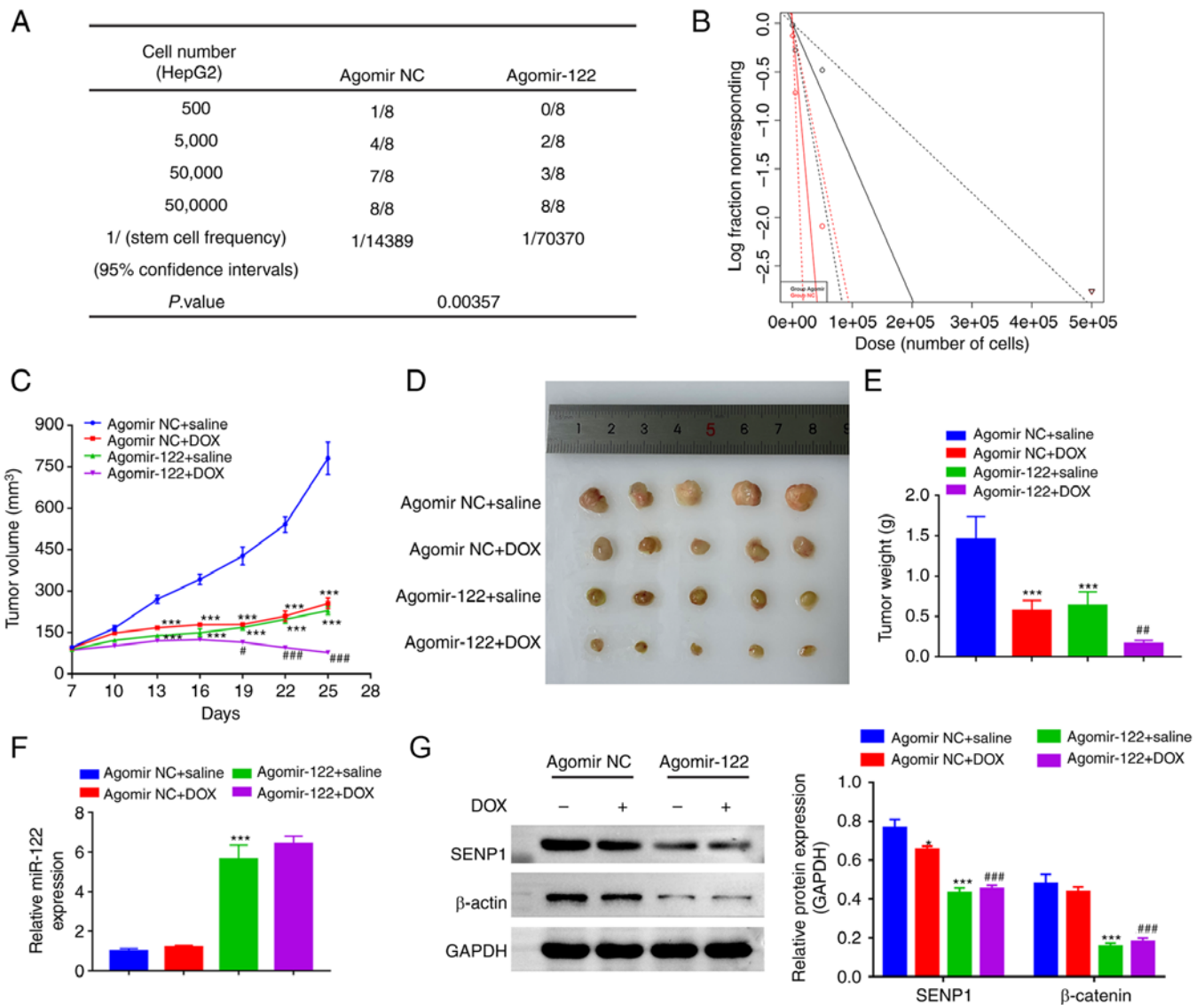
Figure 5. Overexpression of miR-122 reduces the stemness and chemoresistance by downregulating SENP1/β-catenin in liver cancer *in vivo*. The xenograft formation was tested at four dilutions ($5x10^2$, $5x10^3$, $5x10^4$ and $5x10^5$ cells) of HepG2 cells transfected with Agomir NC or Agomir-122. (A) The tumor formation rate was recorded to calculate the confidence intervals for cancer stem cell frequency by extreme limiting dilution analysis. (B) Plot of the log fraction as a function of the implanted HepG2 cell number. The more vertical the line, the higher the percentage of the tumor-initiating cells. HepG2 cells stably transfected with either Agomir NC or Agomir-122 were subcutaneously injected into mice to establish *in vivo* models, and mice were treated with DOX or saline twice a week. (C) Tumor volume was recorded every 3 days for 18 days, 1 week after inoculation. (D) Representative images of tumors formed in each group. (E) Tumor weight in each group. (F) Expression levels of miR-122 in the xenografts were detected by RT-qPCR. (G) The expression levels of SENP1 and β-catenin in the xenografts were detected by western blotting. *$P<0.05$ and ***$P<0.001$ vs. Agomir NC + saline; #$P<0.05$, ##$P<0.005$ and ###$P<0.001$ vs. the Agomir-122 + saline group. DOX, doxorubicin; SENP1, sentrin-specific protease 1; NC, negative control.

prognosis in patients with liver cancer. In addition, it was found to contribute to tumorigenicity and metastasis by promoting the SUMOylation of its target proteins (34). The expression level of SUMO-activating enzyme subunit 1 was also found to be positively associated with liver cancer progression and metastasis (35). Therefore, it was hypothesized in the present study that miR-122 may participate in the malignant processes of liver cancer by regulating SUMOylation. A bioinformatic online tool was first used to screen out the genes involved in SUMOylation targeted by miR-122 in liver cancer.

The present study initially found that SENP1 is a direct target of miR-122, where the miR-122/SENP1 axis was involved in regulating the stemness properties, chemoresistance, proliferation and migration of HepG2 cells.

This was then observed to be at least partially due to the de-SUMOylation function of SENP1 on β-catenin, which is part of the Wnt/β-catenin signaling pathway. To elucidate the role of the miR-122/SENP1 axis in the regulation of the malignant phenotype, the present study modulated their expression by transfecting with miR-122 mimics alone or together with SENP1 overexpression vectors in HepG2 cells. Cancer cells with 'stemness' characteristics are the major drivers of tumor growth, invasion and treatment failure (36). Data in the present study showed that miR-122 negatively regulated the stemness properties, which was demonstrated by the decreased number of tumor spheres formed, decreased expression of stem markers and reduced stem cell population (HepG2 cells expressing the CD24^{+} marker), after miR-122 overexpression

in HepG2 cells. SENP1 co-transfection reversed the aforementioned effects. This suggests that SENP1 can facilitate the stemness property in liver cancer. Similarly, a previous study demonstrated that SENP1 enhanced liver cancer stemness through the de-SUMOylation of hypoxia-inducible factor 1-α under hypoxia (37). Importantly, it was observed that the downregulated self-renewal capacity phenotype of HepG2 cells transfected with miR-122 mimics was reversed after overexpressing SENP1, suggesting that the role of miR-122 in the stemness of liver cancer can be mediated by SENP1.

Consistent with previous reports (37,38), data in the present study showed a significant suppressive effect of miR-122 but an enhancement effect of SENP1 on cell proliferation, migration and multidrug resistance in liver cancer. It has been previously shown that the overexpression of miR-122 can increase both sorafenib (39) and DOX (40) sensitivity in HepG2 cells. Consistent with previous studies, the overexpression of miR-122 increased the sensitivity of HepG2 cells to DOX and sorafenib. However, this effect was reversed by co-transfection with the SENP1 overexpression vector. These data collectively suggest that the miR-122/SENP1 axis can contribute to liver cancer stemness, drug sensitivity, cell proliferation and migration.

The Wnt/β-catenin signaling pathway has been implicated in the occurrence, development and progression of multiple cancers, including liver cancer (41). The important role of the Wnt/β-catenin signaling pathway prompts its consideration as a possible mechanism regulated by the miR-122/SENP1 axis. Results in the present study showed that SENP1 overexpression significantly decreased the SUMOylation of β-catenin, a key molecule in this pathway to increase its stability, rendering the upregulation of β-catenin. By contrast, the overexpression of miR-122 led to a decrease in SENP1 expression, which subsequently increased β-catenin degradation. Subsequently, results from *in vivo* experiments confirmed the findings of the present study that miR-122 could suppress stemness, chemoresistance and β-catenin expression in liver cancer by regulating SENP1.

Collectively, the present study explored the role of the miR-122/SENP1 axis in liver cancer, demonstrating that it can serve a role in the stemness, chemoresistance, cell proliferation and migration of this type. Specifically, it can activate the Wnt/β-catenin signaling pathway through the de-SUMOylation of β-catenin by SENP1. However, all functional studies that determined the effect of the miR-122/SENP1 axis in the present study are based on HepG2 cells in culture. The true biological functions of the miR-122/SENP1 axis and its role in hepatocarcinogenesis should be elucidated in further investigations using knock-out mice in the future.

In summary, the findings of the present study demonstrated that the miR-122/SENP1 axis contributes to the stemness, proliferation, migration and chemoresistance of liver cancer cells by regulating the Wnt/β-catenin signaling pathway through the de-SUMOylation of β-catenin by SENP1. This may serve as a scientific foundation for the potential therapeutic exploitation of the miR-122/SENP1 axis for treating patients with liver cancer.

Acknowledgements

Funding

Availability of data and materials

The datasets used and/or analyzed during the current study are available from the corresponding author on reasonable request.

Author contributions

JD and BW confirm the authenticity of all the raw data. JD, BW and YH designed the study and wrote original draft. JD performed the bioinformatics analysis and animal experiments, and analyzed the data. YH, XC and QSY performed the cell experiments. BW reviewed and edited the manuscript. All authors read and approved the final version of the manuscript.

Ethics approval and consent to participate

All procedures regarding animals in the present study were performed in accordance with relevant guidelines and regulations with the approval by the Institutional Animal Care and Use Committee at the Nan'an District People's Hospital of Chongqing (approval no. 2020-0925). The euthanasia method used was approved by the Institutional Animal Care and Use Committee at the Nan'an District People's Hospital of Chongqing.

Patient consent for publication

Not applicable.

Competing interests

The authors declare that they have no competing interests.

References

1. Sung H, Ferlay J, Siegel RL, Laversanne M, Soerjomataram I, Jemal A and Bray F: Global cancer statistics 2020: GLOBOCAN estimates of incidence and mortality worldwide for 36 cancers in 185 countries. CA Cancer J Clin 71: 209-249, 2021.
2. Lohitesh K, Chowdhury R and Mukherjee S: Resistance a major hindrance to chemotherapy in hepatocellular carcinoma: An insight. Cancer Cell Int 18: 44, 2018.
3. Phi LTH, Sari IN, Yang YG, Lee SH, Jun N, Kim KS, Lee YK and Kwon HY: Cancer stem cells (CSCs) in drug resistance and their therapeutic implications in cancer treatment. Stem Cells Int 2018: 5416923, 2018.
4. Chang JC: Cancer stem cells: Role in tumor growth, recurrence, metastasis, and treatment resistance. Medicine (Baltimore) 95 (1 Suppl 1): S20-S25, 2016.
5. Adhikari AS, Agarwal N and Iwakuma T: Metastatic potential of tumor-initiating cells in solid tumors. Front Biosci (Landmark Ed) 16: 1927-1938, 2011.
6. Lee TK, Cheung VC and Ng IO: Liver tumor-initiating cells as a therapeutic target for hepatocellular carcinoma. Cancer Lett 338: 101-109, 2013.
7. Kim HM, Haraguchi N, Ishii H, Ohkuma M, Okano M, Mimori K, Eguchi H, Yamamoto H, Nagano H, Sekimoto M, *et al*: Increased CD13 expression reduces reactive oxygen species, promoting survival of liver cancer stem cells via an epithelial-mesenchymal transition-like phenomenon. Ann Surg Oncol 19 (Suppl 3): S539-S548, 2012.
8. Subramanian S and Steer CJ: Special issue: MicroRNA regulation in health and disease. Genes (Basel) 10: 457, 2019.

9. Vasudevan S: Posttranscriptional upregulation by microRNAs. Wiley Interdiscip Rev RNA 3: 311-330, 2012.
10. Giovannini C, Minguzzi M, Baglioni M, Fornari F, Giannone F, Ravaioli M, Cescon M, Chieco P, Bolondi L and Gramantieri L: Suppression of p53 by Notch3 is mediated by cyclin G1 and sustained by MDM2 and miR-221 axis in hepatocellular carcinoma. Oncotarget 5: 10607-10620, 2014.
11. Sun C, Yao X, Jiang Q and Sun X: miR-106b targets DAB2 to promote hepatocellular carcinoma cell proliferation and metastasis. Oncol Lett 16: 3063-3069, 2018.
12. Meng F, Henson R, Wehbe-Janek H, Ghoshal K, Jacob ST and Patel T: MicroRNA-21 regulates expression of the PTEN tumor suppressor gene in human hepatocellular cancer. Gastroenterology 133: 647-658, 2007.
13. Simerzin A, Zorde-Khvalevsky E, Rivkin M, Adar R, Zucman-Rossi J, Couchy G, Roskams T, Govaere O, Oren M, Giladi H and Galun E: The liver-specific microRNA-122*, the complementary strand of microRNA-122, acts as a tumor suppressor by modulating the p53/mouse double minute 2 homolog circuitry. Hepatology 64: 1623-1636, 2016.
14. Girard M, Jacquemin E, Munnich A, Lyonnet S and Henrion-Caude A: miR-122, a paradigm for the role of microRNAs in the liver. J Hepatol 48: 648-656, 2008.
15. Cheung O, Puri P, Eicken C, Contos MJ, Mirshahi F, Maher JW, Kellum JM, Min H, Luketic VA and Sanyal AJ: Nonalcoholic steatohepatitis is associated with altered hepatic MicroRNA expression. Hepatology 48: 1810-1820, 2008.
16. Hsu SH, Wang B, Kota J, Yu J, Costinean S, Kutay H, Yu L, Bai S, La Perle K, Chivukula RR, *et al*: Essential metabolic, anti-inflammatory, and anti-tumorigenic functions of miR-122 in liver. J Clin Invest 122: 2871-2883, 2012.
17. Tsai WC, Hsu SD, Hsu CS, Lai TC, Chen SJ, Shen R, Huang Y, Chen HC, Lee CH, Tsai TF, *et al*: MicroRNA-122 plays a critical role in liver homeostasis and hepatocarcinogenesis. J Clin Invest 122: 2884-2897, 2012.
18. Xu Y, Bu X, Dai C and Shang C: High serum microRNA-122 level is independently associated with higher overall survival rate in hepatocellular carcinoma patients. Tumour Biol 36: 4773-4776, 2015.
19. Kim SS, Nam JS, Cho HJ, Won JH, Kim JW, Ji JH, Yang MJ, Park JH, Noh CK, Shin SJ, *et al*: Plasma microRNA-122 as a predictive marker for treatment response following transarterial chemoembolization in patients with hepatocellular carcinoma. J Gastroenterol Hepatol 32: 199-207, 2017.
20. Celen AB and Sahin U: Sumoylation on its 25th anniversary: Mechanisms, pathology, and emerging concepts. FEBS J 287: 3110-3140, 2020.
21. Zubiete-Franco I, García-Rodríguez JL, Lopitz-Otsoa F, Serrano-Macia M, Simon J, Fernández-Tussy P, Barbier-Torres L, Fernández-Ramos D, Gutiérrez-de-Juan V, López de Davalillo S, *et al*: SUMOylation regulates LKB1 localization and its oncogenic activity in liver cancer. EBioMedicine 40: 406-421, 2019.
22. Qin Y, Bao H, Pan Y, Yin M, Liu Y, Wu S and Li H: SUMOylation alterations are associated with multidrug resistance in hepatocellular carcinoma. Mol Med Rep 9: 877-881, 2014.
23. Li JH, Liu S, Zhou H, Qu LH and Yang JH: starBase v2.0: Decoding miRNA-ceRNA, miRNA-ncRNA and protein-RNA interaction networks from large-scale CLIP-Seq data. Nucleic Acids Res 42 (Database Issue): D92-D97, 2014.
24. Livak KJ and Schmittgen TD: Analysis of relative gene expression data using real-time quantitative PCR and the 2(-Delta Delta C(T)) method. Methods 25: 402-408, 2001.
25. Hu Y and Smyth GK: ELDA: Extreme limiting dilution analysis for comparing depleted and enriched populations in stem cell and other assays. J Immunol Methods 347: 70-78, 2009.
26. Tomasi ML and Ramani K: SUMOylation and phosphorylation cross-talk in hepatocellular carcinoma. Transl Gastroenterol Hepatol 3: 20, 2018.

27. Yuan H, Lu Y, Chan YT, Zhang C, Wang N and Feng Y: The role of protein SUMOylation in human hepatocellular carcinoma: A potential target of new drug discovery and development. Cancers (Basel) 13: 5700, 2021.
28. Mohammed MK, Shao C, Wang J, Wei Q, Wang X, Collier Z, Tang S, Liu H, Zhang F, Huang J, *et al*: Wnt/β-catenin signaling plays an ever-expanding role in stem cell self-renewal, tumorigenesis and cancer chemoresistance. Genes Dis 3: 11-40, 2016.
29. Cao W, Chen HD, Yu YW, Li N and Chen WQ: Changing profiles of cancer burden worldwide and in China: A secondary analysis of the global cancer statistics 2020. Chin Med J (Engl) 134: 783-791, 2021.
30. Chen Z, Xie H, Hu M, Huang T, Hu Y, Sang N and Zhao Y: Recent progress in treatment of hepatocellular carcinoma. Am J Cancer Res 10: 2993-3036, 2020.
31. Gramantieri L, Fornari F, Callegari E, Sabbioni S, Lanza G, Croce CM, Bolondi L and Negrini M: MicroRNA involvement in hepatocellular carcinoma. J Cell Mol Med 12: 2189-2204, 2008.
32. Geiss-Friedlander R and Melchior F: Concepts in sumoylation: A decade on. Nat Rev Mol Cell Biol 8: 947-956, 2007.
33. Yeh ETH: SUMOylation and De-SUMOylation: Wrestling with life's processes. J Biol Chem 284: 8223-8227, 2009.
34. Liu Q, Zhou B, Liao R, Zhou X and Yan X: PIAS4, upregulated in hepatocellular carcinoma, promotes tumorigenicity and metastasis. J Cell Biochem 121: 3372-3381, 2020.
35. Ong JR, Bamodu OA, Khang NV, Lin YK, Yeh CT, Lee WH and Cherng YG: SUMO-activating enzyme subunit 1 (SAE1) is a promising diagnostic cancer metabolism biomarker of hepatocellular carcinoma. Cells 10: 178, 2021.
36. Tsui YM, Chan LK and Ng IO: Cancer stemness in hepatocellular carcinoma: Mechanisms and translational potential. Br J Cancer 122: 1428-1440, 2020.
37. Cui CP, Wong CC, Kai AK, Ho DW, Lau EY, Tsui YM, Chan LK, Cheung TT, Chok KS, Chan ACY, *et al*: SENP1 promotes hypoxia-induced cancer stemness by HIF-1α deSUMOylation and SENP1/HIF-1α positive feedback loop. Gut 66: 2149-2159, 2017.
38. Wang N, Wang Q, Shen D, Sun X, Cao X and Wu D: Downregulation of microRNA-122 promotes proliferation, migration, and invasion of human hepatocellular carcinoma cells by activating epithelial-mesenchymal transition. Onco Targets Ther 9: 2035-2047, 2016.
39. Turato C, Fornari F, Pollutri D, Fassan M, Quarta S, Villano G, Ruvoletto M, Bolondi L, Gramantieri L and Pontisso P: MiR-122 targets SerpinB3 and is involved in sorafenib resistance in hepatocellular carcinoma. J Clin Med 8: 171, 2019.
40. Fornari F, Gramantieri L, Giovannini C, Veronese A, Ferracin M, Sabbioni S, Calin GA, Grazi GL, Croce CM, Tavolari S, *et al*: MiR-122/cyclin G1 interaction modulates p53 activity and affects doxorubicin sensitivity of human hepatocarcinoma cells. Cancer Res 69: 5761-5767, 2009.
41. Vilchez V, Turcios L, Marti F and Gedaly R: Targeting Wnt/β-catenin pathway in hepatocellular carcinoma treatment. World J Gastroenterol 22: 823-832, 2016.